Mechanism of interaction of optimized *Limulus*-derived cyclic peptides with endotoxins: thermodynamic, biophysical and microbiological analysis

Jörg ANDRÄ*, Jörg HOWE*, Patrick GARIDEL†, Manfred RÖSSLE‡, Walter RICHTER§, José LEIVA-LEÓN‖, Ignacio MORIYON‖, Rainer BARTELS*, Thomas GUTSMANN* and Klaus BRANDENBURG*[1]

*Forschungszentrum Borstel, Leibniz-Zentrum für Medizin und Biowissenschaften, Biophysik, Parkallee 10, 23845 Borstel, Germany, †Institut für Physikalische Chemie, Martin-Luther-Universität Halle-Wittenberg, Mühlpforte 1, 06108 Halle, Germany, ‡European Molecular Biology Laboratory c/o DESY, Notkestr. 85, 22603 Hamburg, Germany, §Friedrich-Schiller-Universität Jena, Elektronenmikroskopisches Zentrum der Medizinischen Fakultät, Ziegelmühlenweg 1, 07740 Jena, Germany, and ‖Departamento de Microbiologia, Universidad de Navarra, Irunlarrea 1, 31008 Pamplona, Spain

On the basis of formerly investigated peptides corresponding to the endotoxin-binding domain from LALF [*Limulus* anti-LPS (lipopolysaccharide) factor], a protein from *Limulus polyphemus*, we have designed and synthesized peptides of different lengths with the aim of obtaining potential therapeutic agents against septic shock syndrome. For an understanding of the mechanisms of action, we performed a detailed physicochemical and biophysical analysis of the interaction of rough mutant LPS with these peptides by applying FTIR (Fourier-transform infrared) spectroscopy, SAXS (small-angle X-ray scattering), calorimetric techniques [DSC (differential scanning calorimetry) and ITC (isothermal titration calorimetry)] and FFTEM (freeze-fracture transmission electron microscopy). Also, the action of the peptides on bacteria of different origin in microbial assays was investigated. Using FTIR and DSC, our results indicated a strong fluidization of the lipid A acyl chains due to peptide binding, with a decrease in the endothermic melting enthalpy change of the acyl chains down to a complete disappearance in the 1:0.5 to 1:2 [LPS]:[peptide] molar ratio range. Via ITC, it was deduced that the binding is a clearly exothermic process which becomes saturated at a 1:0.5 to 1:2 [LPS]:[peptide] molar ratio range. The results obtained with SAXS indicated a drastic change of the aggregate structures of LPS into a multilamellar stack, which was visualized in electron micrographs as hundreds of lamellar layers. This can be directly correlated with the inhibition of the LPS-induced production of tumour necrosis factor α in human mononuclear cells, but not with the action of the peptides on bacteria.

Key words: antimicrobial peptide, cytokine induction, Fourier-transform infrared (FTIR), *Limulus* test, lipopolysaccharide neutralization (LPS neutralization), small-angle X-ray scattering (SAXS).

INTRODUCTION

Cell wall-bound molecules of bacteria such as LPS (lipopolysaccharide) may be released into the environment by the attack of the immune system or simply due to cell division, and may then interact with serum or membrane proteins such as soluble or membrane-bound LBP (LPS-binding protein) and CD14 [1–3]. In a following step, this interaction may then promote specific receptors such as TLR4 (Toll-like receptor 4)/MD2, which eventually leads to cell activation [4,5]. At low and moderate concentrations of LPS the subsequent inflammation reaction is beneficial for the host, but at higher LPS concentrations the cascade of molecular and cellular events may lead to endotoxic shock syndrome with high mortality, particularly in critical care units [6,7]. It is known that lipid A, the hydrophobic moiety anchoring LPS into the outer membrane of Gram-negative bacteria, constitutes the 'endotoxic principle' of LPS. Enterobacterial lipid A consists of a diglucosamine backbone phosphorylated at positions 1 and 4′ to which mainly six acyl chains are linked at positions 2,3 and 2′,3′. Furthermore, in all LPS chemotypes to lipid A two special monosaccharides, Kdo (2-keto-3-deoxyoctonate), are linked, which are negatively charged due to their carboxylate groups. Thus a necessary condition for LPS neutralization is the presence of positive charges, which can be achieved by the use of cationic peptides [8]. Previously, we have synthesized peptides based on the LALF (*Limulus*-anti-LPS-factor) from the horseshoe crab *Limulus polyphemus* [9]. These partial structures containing the LPS-binding domain or parts of it were found to have high endotoxin-binding and neutralizing activities, comparable with that of the parent recombinant rLALF protein [also called ENP (endotoxin-neutralizing protein)] [10], and to be non-toxic for erythrocytes or cultured human monocytes [11].

Based on these peptides, we have synthesized a number of cyclic peptides and have performed a detailed biophysical characterization of their interaction with mutant Ra LPS from *Salmonella* Minnesota strain R60, which has well-defined chemical structure and corresponds to the active unit in heterogeneous mixtures of wild-type LPS [12]. In some cases also deep rough mutant Re LPS (from *Salmonella* Minnesota strain R595) as well as the 'endotoxic principle' lipid A were used. Information was obtained with regard to changes caused by peptide binding in the LPS/lipid A aggregate structure, phase transition behaviour (temperature

Abbreviations used: cfu, colony-forming units; DSC, differential scanning calorimetry; FFTEM, freeze-fracture transmission electron microscopy; Fmoc, fluoren-9-ylmethoxycarbonyl; FRET, fluorescence resonance energy transfer; FTIR, Fourier-transform infrared; ITC, isothermal titration calorimetry; LPS, lipopolysaccharide; LALF, *Limulus*-anti-LPS factor; cLALF, cyclic LALF; LB, Luria–Bertani; LBP, LPS-binding protein; MBC, minimal bactericidal concentration; MIC, minimal inhibitory concentration; MNC, mononuclear cells; NBD, 7-nitrobenz-2-oxa-1,3-diazole; PE, phosphatidylethanolamine; PMB, polymyxin B; PS, phosphatidylserine; Rh, rhodamine; RP-HPLC, reversed-phase HPLC; SAXS, small-angle X-ray scattering; TFA, trifluoroacetic acid; TLR4, Toll-like receptor 4; TNFα, tumour necrosis factor α.

[1] To whom correspondence should be addressed (email kbranden@fz-borstel.de).

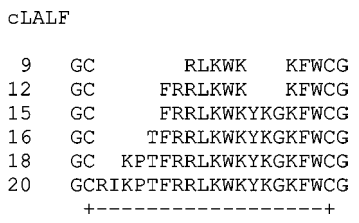

Figure 1 Amino acid sequences of the synthesized cyclic LALF peptides

The cyclation is performed between the two cysteine residues as indicated for cLALF20.

and enthalpy), mobilities of the acyl chains in the single phases, the binding epitopes, in particular the negative charges in lipid A, and the binding stoichiometry. Correlation of these results with data on the cytokine-inhibiting capacity of the peptides and their antimicrobial activity clearly established that the neutralizing activity of the peptides was linked to their affinity for LPS and to their ability to incorporate into target cell membranes. These results allow an understanding of the mechanism of the endotoxin–peptide interaction.

EXPERIMENTAL

Lipids

LPSs from rough mutant Re and Ra from *Salmonella* Minnesota (strains R595 and R60 respectively) were extracted by the chloroform/light petroleum method [13] from bacteria grown at 37 °C, purified, and freeze-dried. Free lipid A was isolated by acetate buffer treatment of LPS R595. After isolation, the resulting lipid A was purified and converted into its triethylamine salt. Results of all the standard assays performed on the purified LPS and lipid A (analysis of the amount of glucosamine and total and organic phosphate, and the distribution of the fatty acid residues) were in good agreement with the chemical properties expected for LPS R595 and R60, whose molecular structure has already been solved [14].

Preparation of endotoxin aggregates

LPS or lipid A was solubilized in the appropriate buffer (lipid concentration 1–10 mM, depending on the applied technique), extensively vortex-mixed, sonicated for 30 min in a water bath, and subjected to several temperature cycles between 20 and 60 °C. Finally, the lipid suspension was incubated at 4 °C for at least 12 h before use.

Peptides

Peptides containing the described LPS-binding domain of LALF [15] termed cLALF9, 12, 15, 16, 18 and 20 (where c is cyclic; for structures, see Figure 1) were synthesized with an amidated C-terminus by the solid-phase peptide synthesis technique on an automatic peptide synthesizer (model 433 A; Applied Biosystems) on the standard Fmoc (fluoren-9-ylmethoxycarbonyl)-amide resin according to the FastMoc synthesis protocol of the manufacturer. The N-terminal Fmoc group was removed from the peptide resin and the peptide was deprotected and cleaved with 90 % (v/v) TFA (trifluoroacetic acid), 5 % anisole, 2 % thioanisole and 3 % DTT (dithiothreitol) for 3 h at room temperature (22 °C). After cleavage the suspension was filtered and the soluble peptides were precipitated with ice-cold diethyl ether followed by centrifugation and extensive washing with diethyl ether. Peptides were purified by RP-HPLC (reversed-phase HPLC) using an Aqua-C_{18} column (Phenomenex). Elution was done by using a gradient of 0–70 % acetonitrile in 0.1 % TFA. Cyclation via cysteine residues was achieved by incubating the peptides in 10 % (v/v) DMSO for 24 h at room temperature. The peptides were then again purified by RP-HPLC to purities above 95 %. Purity was determined by MALDI–TOF-MS (matrix-assisted laser-desorption–time-of-flight MS; Bruker). In some cases, peptide cLALF22, corresponding to the complete LPS-binding domain of LALF [16], was used. It differs from cLALF20 by the additional amino acids HY between the GC and the RI residues [third and fourth amino acid from the N-terminus (Figure 1)].

FTIR (Fourier-transform infrared) spectroscopy

The IR spectroscopic measurements were performed on an IFS-55 spectrometer (Bruker). Samples, dissolved in 20 mM Hepes buffer (pH 7.0), were placed in a CaF_2 cuvette with a 12.5 μm Teflon spacer. Temperature scans were performed automatically between 10 and 70 °C with a heating rate of 0.6 °C min^{-1}. Every 3 °C, 50 interferograms were accumulated, apodized, Fourier-transformed, and converted into absorbance spectra.

DSC (differential scanning calorimetry)

DSC measurements were performed with VP-DSC and MC-2 calorimeters (Microcal) at a heating and cooling rate of 1 °C min^{-1}. The DSC samples were prepared by dispersing a known amount ($\sim$3 mg/ml) in 10 mM PBS buffer at pH 7.4. The samples were hydrated in the liquid crystalline phase by vortex-mixing. Prior to the measurements the DSC samples were stored for a defined time at 4 °C (see below). The measurements were performed in the temperature interval from 5 to 95 °C. In the Figures only the temperature ranges where phase transitions were observed are shown. Five consecutive heating and cooling scans checked the reproducibility of the DSC experiments of each sample [17]. The accuracy of the DSC experiments was $\pm$0.1 °C for the main phase transition temperatures and $\pm$1 kJ/mol for the main phase transition enthalpy. The DSC data were analysed using the Origin software. The phase transition enthalpy was obtained by integrating the area under the heat capacity curve [18].

ITC (isothermal titration calorimetry)

Microcalorimetric measurements of peptide binding to endotoxins were performed on an MCS isothermal titration calorimeter (Microcal) at 37 °C as previously described [19]. Endotoxin samples (0.05–0.15 mM), prepared as described above, were dispensed into the microcalorimetric cell (volume 1.3 ml) and peptide solutions in the concentration range 0.5–5 mM were filled into the syringe compartment (volume 100 μl), each after thorough degassing of the suspensions. After temperature equilibration, the peptides were titrated in 3 μl portions every 5 min into the lipid-containing cell under constant stirring, and the measured heat of interaction after each injection measured by the ITC instrument was plotted against time. As addition of the peptides into pure buffer solution gave only negligible heat of dilution, the total heat signal from each experiment was determined as the area under the respective single peaks and plotted against the [peptide]:[lipid] molar ratio. Since the instrument works in temperature equilibrium at a constant 'current feedback' corresponding to a power of approx. 74 μW, the occurrence of an exothermic reaction leads to a lowering of this current, whereas an endothermic reaction causes an increase. All titration curves were repeated at least twice.

X-ray diffraction

X-ray diffraction measurements were performed at the EMBL (European Molecular Biology Laboratory) outstation at the Hamburg synchrotron radiation facility HASYLAB using the double-focusing monochromator–mirror camera X33 [20]. Diffraction patterns in the range of the scattering vector $0.1 < s < 4.5\ nm^{-1}$ ($s = 2\sin\theta/\lambda$, where 2θ is the scattering angle and λ is the wavelength = 0.15 nm) were recorded at 40 °C with exposure times of 1 min using an image plate detector with online readout (MAR345; MarResearch). The *s*-axis was calibrated with Ag-Behenate, which has a periodicity of 58.4 nm. The diffraction patterns were evaluated as described previously [21] assigning the spacing ratios of the main scattering maxima to defined three-dimensional structures. The lamellar and cubic structures are most relevant here. They are characterized by the following features. (i) Lamellar: the reflections are grouped in equidistant ratios, i.e., 1, 1:2, 1:3, 1:4 etc. of the lamellar repeat distance d_l. (ii) Cubic: the different space groups of these non-lamellar three-dimensional structures differ in the ratio of their spacings. The relation between reciprocal spacing $s_{hkl} = 1/d_{hkl}$ and lattice constant a is

$$s_{hkl} = [(h^2 + k^2 + l^2)/a]^{1/2}$$

(hkl = Miller indices of the corresponding set of planes).

FFTEM (freeze-fracture transmission electron microscopy)

LPS and LPS/peptide samples were prepared as described above with around 90 % water content (3–5 mg/30 μl). For freeze-fracturing, the samples, copper sandwich profiles, and instruments for manipulation were incubated at room temperature or at 40 °C. A small amount of the sample was sandwiched between two copper profiles as used for the double-replica technique and frozen by plunging the sandwiches immediately into liquified propane cooled in liquid nitrogen. Fracturing and replication were performed at −150 °C in a BAF 400T freeze-fracture device (BAL-TEC) equipped with electron guns and a film sheet thickness monitor. The replicas were placed on copper grids, cleaned with a chloroform/methanol mixture, and examined in an EM900 electron microscope (Zeiss).

FRET (fluorescence resonance energy transfer)

The FRET technique was used as a probe dilution assay [22] to obtain information on the intercalation of the peptides in the absence and presence of LPS into liposomes made from PS (phosphatidylserine). For the FRET experiments, liposomes were double-labelled with NBD (7-nitrobenz-2-oxa-1,3-diazole)-PE (phosphatidylethanolamine) and Rh (rhodamine)-PE in chloroform [PS]:[NBD-PE]:[Rh-PE] at 100:1:1 molar ratios. The solvent was evaporated under a stream of nitrogen, the lipids resuspended in PBS, mixed thoroughly, and sonicated with a Branson sonicator for 1 min (1 ml solution). Subsequently, the preparation was temperature-cycled at least twice between 4 and 56 °C, each cycle followed by intense vortex-mixing for a few minutes, and then stored at 4 °C for at least 12 h prior to measurement. A preparation of 900 μl of the double-labelled liposomes (10^{-5} M) at 37 °C was excited at 470 nm (λ_{ex} of NBD-PE), and the intensities of the emission light of the donor NBD-PE (531 nm) and acceptor Rh-PE (593 nm) were measured simultaneously on the fluorescence spectrometer SPEX F1T11 (SPEX Instruments). The peptides cLALF (final concentration 1 μM) were added to liposomes after 50 s, and LPS after 100 s (cLALF/LPS 1:1 molar ratio). Furthermore, co-incubated (LPS + cLALF) samples were added after 50 s. Since FRET spectroscopy is used here as a probe dilution assay, intercalation of molecules causes an increase in the distance between donor and acceptor in the liposomes and, thus, leads to a reduced energy transfer. This again causes an increase in the donor and decrease in the acceptor intensities. For a qualitative analysis of experiments, the quotient of the intensities of the donor dye and the acceptor dye are plotted against time (denoted in the following as the FRET signal). The results shown are representative of three independent experiments.

Stimulation of human MNCs (mononuclear cells) by LPS

MNCs were isolated from heparinized blood of healthy human donors as described previously [23]. The cells were resuspended in medium (RPMI 1640) and their number was equilibrated at 5×10^6 cells/ml. For stimulation, 200 μl of MNC (1×10^6 cells) was transferred into each well of a 96-well culture plate. LPS and peptide/LPS mixtures were incubated for 30 min at 37 °C, and added to the cultures at 20 μl per well. The cultures were incubated for 4 h at 37 °C under 5 % CO_2. Supernatants were collected after centrifugation of the culture plates for 10 min at 400 ***g*** and stored at −20 °C until determination of TNFα (tumour necrosis factor α) content. Immunological determination of TNFα was carried out in a Sandwich ELISA using a monoclonal antibody against TNF (clone 6b from Intex AG) and was described earlier in detail [23].

Assays for cytotoxicity

Cytotoxicity of the peptides was determined against HeLa cells in medium by an MTT [3-(4,5-dimethylthiazol-2-yl)-2,5-diphenyl-2*H*-tetrazolium bromide] assay as described previously [24].

Assay for haemolytic activity

Haemolytic activity of the peptides against human erythrocytes was determined as described previously [24]. Briefly, peptides were incubated with a freshly prepared erythrocyte suspension from human blood (5 % of normal haematocrit) in 10 mM PBS (pH 7.2), for 30 min at 37 °C. Released Hb was determined photometrically at 412 nm.

Assays for antibacterial activities

The antibacterial activity of the peptides was determined by microdilution susceptibility assays performed (i) in standard Müller–Hinton broth or (ii) in 20 mM Hepes buffer (pH 7.0) supplemented with 10 % LB (Luria–Bertani) broth.

Assay in Müller–Hinton broth

Susceptibility testing was performed following the recommendations of the CLSI [Clinical Standards Institute; formerly NCCLS (National Committee for Clinical Laboratory Standards)] (Standards, 2000) [25]. Peptides [2 mg/ml in 4 mM Hepes (pH 7.2)] were two-fold diluted in Müller–Hinton broth (pH 7.3) (Difco Laboratories) in 96-well microtitre plates (TPP) to obtain concentrations from 512 to 0.25 μg/ml in a volume of 100 μl. Bacteria were grown on Müller–Hinton agar plates (bioMérieux) for 1–3 days depending on the growth rate of the bacteria, suspended in 2 ml of 0.9 % saline and adjusted to 10^8 cfu (colony-forming units)/ml. The bacterial suspension was diluted 100-fold in Müller–Hinton broth, and 0.1 ml of this new dilution (10^5 cfu) was added to the peptide dilutions. The microtitre plates were

incubated at 37 °C for 24 h. The MIC (minimal inhibitory concentration) of each peptide against a given bacterial strain was regarded as the minimal concentration of the peptide that prevents the growth of that organism 24 h after inoculation. The bactericidal effect of the peptides was determined, after 24 h incubation at 37 °C, by plating 10 μl of the content of non-cloudy wells on to Müller–Hinton agar plates. Plates were incubated at 37 °C for 1–5 days, and a viable count was performed. The MBC (minimal bactericidal concentration) of each peptide for a given bacterial strain was regarded as the minimal concentration of the peptide that kills 99.9 % of the cfu present in the final inoculum.

Assays in LB medium/buffer

Peptides (dissolved in 20 mM Hepes, pH 7.0) were 2-fold diluted in the same buffer in 96-well microtitre plates (Greiner). Subsequently, a suspension of exponential-phase bacteria in LB was added (10 μl, containing 10^4 cfu) to the peptide solution (90 μl). The plates were incubated overnight in a wet chamber at 37 °C under constant shaking and bacterial growth was monitored by measuring the absorbance at 620 nm in a microtitre plate reader (Rainbow; Tecan). The MIC was defined as the lowest peptide concentration at which no bacterial growth was measurable. Portions of each well (10 μl) were diluted with 90 μl of Hepes buffer, plated out in duplicate on to LB-agar plates, incubated overnight at 37 °C, and bacterial colonies were counted. The MBC was defined as the peptide concentration at which no colony growth was observed. Experiments were performed at least twice in duplicates.

RESULTS

Various physical techniques were applied to characterize the interaction of LPS Ra, in some cases also of LPS Re and lipid A as endotoxic principle, with the peptides.

Gel-to-liquid crystalline phase transition behaviour

The influence of the peptides on the gel-to-liquid crystalline $\beta \leftrightarrow \alpha$ phase behaviour of the acyl chains of LPS Ra, as studied by DSC, showed for all peptides strong interaction with the LPS aggregates (Figure 2). For all peptides, the endothermic melting enthalpy of the hydrocarbon chains of LPS decreased with increasing peptide concentration and vanished at equimolar ratios. The peptides cLALF15 and 20 acted strongest, for which the endotherm disappears at an [LPS]:[peptide] 2:1 molar ratio. This became evident more clearly when the enthalpy change ΔH of the acyl chain melting transition was plotted against the [LPS Ra]:[peptide] molar ratio (Figure 3). From these results, it can be concluded that, besides the electrostatic attraction between the positive charges of the peptide and the negative charges of LPS, a hydrophobic interaction also takes place, leading to a complete abolishment of the chain melting. This chain melting-abolishing effect can be interpreted in two ways, as fluidization of the hydrocarbon chains at low temperatures or as maintaining of the gel phase up to high temperatures. To differentiate between these possibilities, FTIR was applied by monitoring the peak position of the symmetric stretching vibration of the hydrocarbon chains ν_s (CH_2) against temperature. This is plotted in Figure 4 for the interaction of LPS Ra with cLALF9, 15, 18 and 20. As it is known that the peak position of ν_s (CH_2) lies around 2850 cm^{-1} in the gel and around 2852.5–2853 cm^{-1} in the liquid crystalline phases [26], it can be deduced from Figure 4 that the action of the peptides led to a fluidization of the acyl chains in the gel phase, connected

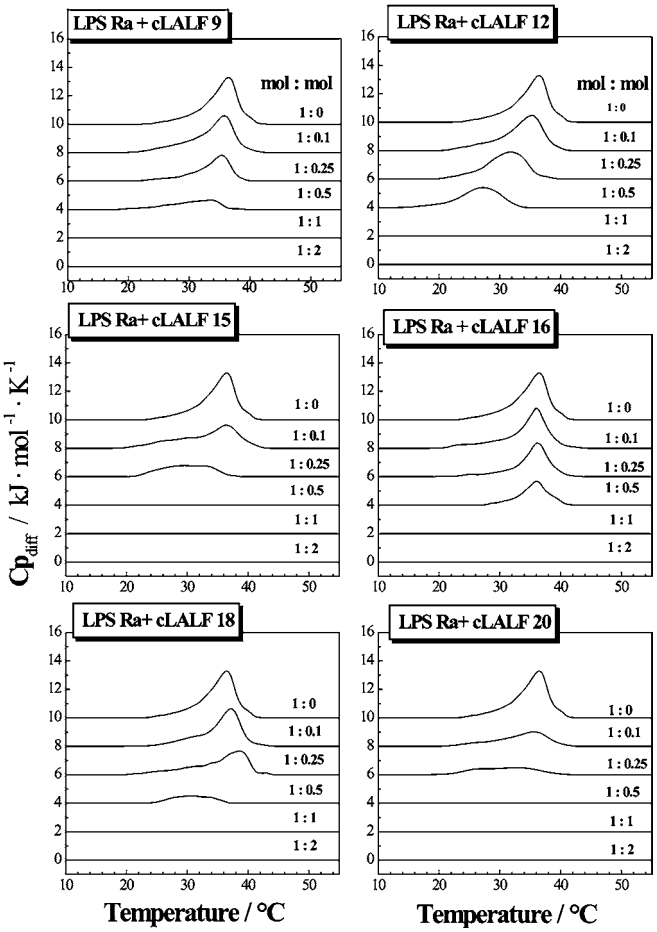

Figure 2 DSC heating-scans of LPS R60 in the presence of different concentrations of peptides cLALF9–20

The specific excess heat capacity, $C_{p\,diff}$, of the calorimetric sample cell as compared with the reference cell is plotted against temperature. The peak positions directed upwards are characteristic for endothermic chain melting processes.

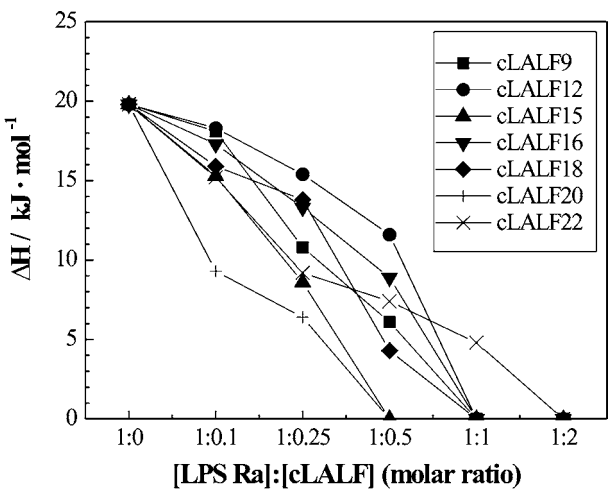

Figure 3 Calorimetrically determined enthalpy change, ΔH_c, against [LPS]:[peptide] molar ratio from DSC scans of Figure 2

with a strong reduction of the phase-transition temperature T_c. In particular at 37 °C, a dramatic increase in the wavenumber values to more than 2853 cm^{-1} took place. Nevertheless, the change of

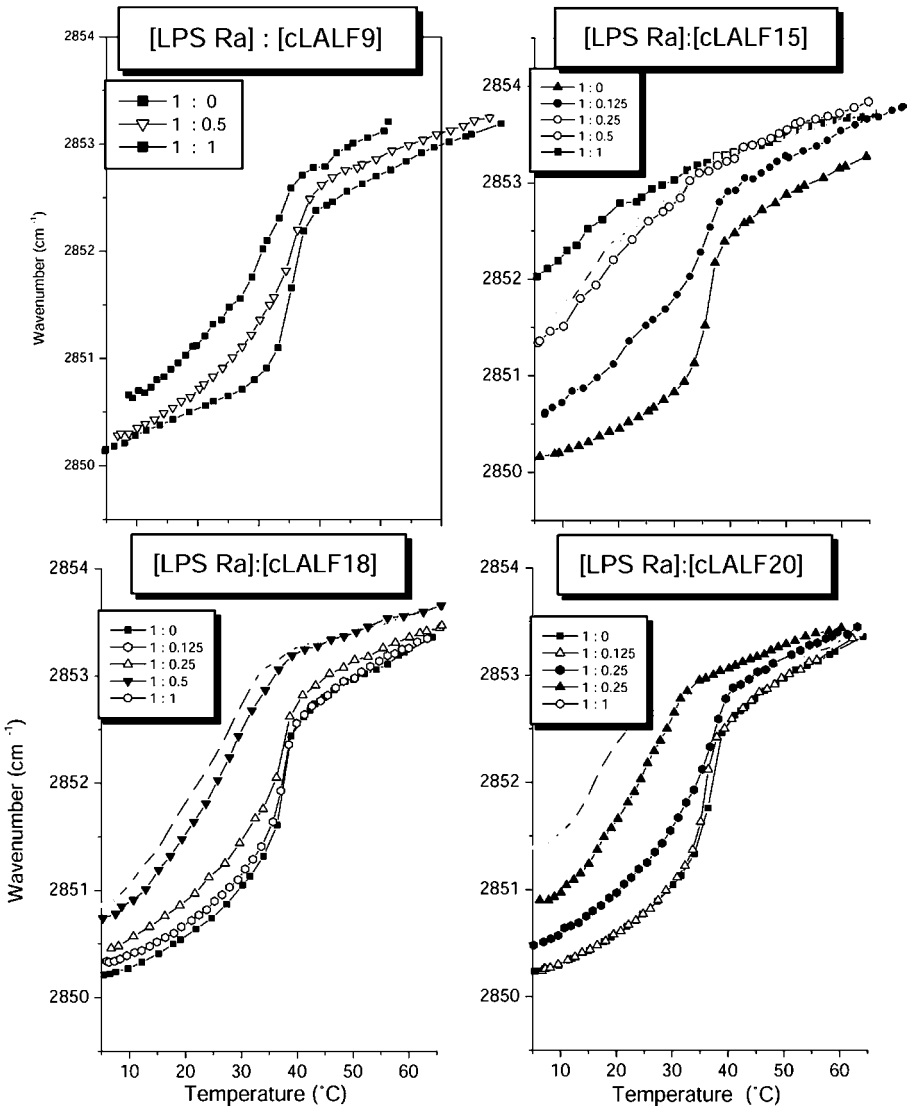

Figure 4 Gel-to-liquid crystalline phase behaviour of the hydrocarbon chains in the lipid A moiety of LPS in the absence and presence of cLALF9, 15, 18 and 20 in FTIR experiments

Plotted is the peak position of the symmetric stretching vibration of the methylene groups against temperature. The gel phase corresponds to wavenumber values around 2850 cm^{-1} and the liquid crystalline phase corresponds to values around 2852.5–2853.0 cm^{-1}.

the wavenumbers over a broad temperature range (10–40 °C) for the LPS/peptide mixtures at 1:0.5 and 1:1 molar ratio is a hint that in the DSC scans this transition cannot be observed enthalpically.

Binding experiments

ITC is the method of choice to determine the enthalpy change caused by the peptide–LPS binding and its stoichiometry. For this, 0.05 mM LPS Ra dispersions were titrated with 2 mM peptide solutions. One original titration is shown in Figure 5(A) for LPS Ra and cLALF20 showing an exothermic reaction (decrease of feedback power to compensate for the temperature increase in the sample cell). A saturation is observed after the tenth injection (after approx. 2500 s). When plotting the integrated areas of the enthalpy curves (enthalpy change ΔH_c) against [LPS]:[peptide] molar ratios (Figure 5B), it can be deduced that (i) for all peptides the negative enthalpy change ΔH_c corresponds to exothermic reactions, and (ii) the titrations indicate a two-step process. Thus, for cLALF15, minima in the curve were observed at [LPS]:[peptide] = 0.3 and 1.6 respectively. Furthermore, binding saturation took place at the highest molar ratio for cLALF9 ([LPS]:[peptide] = 2) and was lowest for cLALF20 ([LPS]:[peptide] < 1). The saturation values for the other peptides were intermediate between these two.

Ultrastructural analysis

It has been shown that non-lamellar aggregate structures for LPS (in particular the lipid A part of LPS) are essential for the expression of biological activity [27]. We thus applied synchrotron radiation small-angle X-ray diffraction to determine the aggregate structure of LPS in the presence of the peptides. For the latter, we used deep rough mutant LPS Re with a short core oligosaccharide rather than LPS Ra with the complete core oligosaccharide [28], since the spectra of the former are more readily resolvable and interpretable [29,30]. The diffraction patterns for pure LPS Re

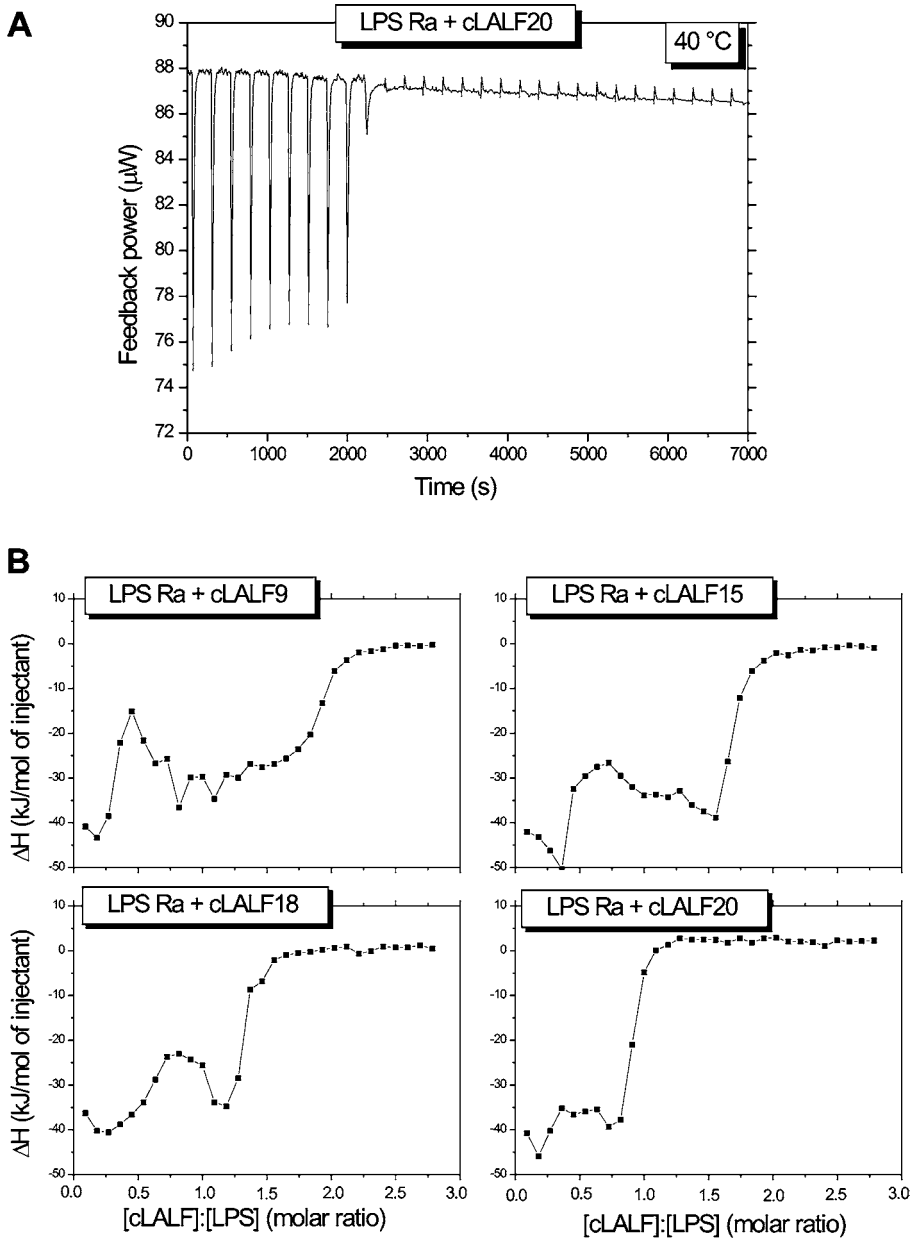

Figure 5 Isothermal calorimetric titration of 0.05 mM LPS Ra with 2 mM cLALF peptides (30 × 3 μl every 5 min)

(**A**) Original titration of LPS with cLALF20 (raw data). (**B**) Integrated peak areas of the single titrations according to (**A**) against [peptide]:[LPS] molar ratios for cLALF9, 15, 18 and 20.

were indicative of the existence of a mixed unilamellar/cubic structure, as described earlier [29] (results not shown). In the presence of the peptides cLALF18 and 20, the diffraction patterns in the temperature range 5–60 °C were characteristic for the existence of multilamellar structures, deduced from the occurrence of reflections at equidistant ratios (Figure 6A). For the LPS–cLALF18 complex, a closer look at the patterns at 40 °C (Figure 6B) showed a main periodicity at 6.62 nm and three further reflections corresponding to the higher orders, and some smaller peaks. These were more readily expressed for the LPS–cLALF20 complex, showing a second lamellar periodicity at 5.32 nm and its second order at 2.64 nm (Figure 6B, bottom).

Regarding the periodicities, it has been shown for LPS Re that these values lie in the range 5.90–6.40 nm in cases in which this LPS adopts a multilamellar structure (in the presence of Mg^{2+} or at low water content, [29]). Therefore the addition of cLALF18 apparently leads to an increase in lamellar stacking periodicity, whereas that of cLALF20 does not, or is even decreased reflecting the lower value of the periodicity.

Also, the aggregate structures of free lipid A (as 'endotoxic principle') in the presence of cLALF18 and 20 were elucidated (results not shown). Similar to the case of LPS Re, the reflections at equidistant ratios indicated multilamellar structures. The values of the periodicities (6.49 nm), however, were very high, considering the fact that the values for pure lipid A are approx. 4.9–5.3 nm [31]. Thus, in this case a strong increase of the water layer between neighbouring bilayers due to peptide binding took place (swelling of the interlamellar repeat).

For the system LPS Re–cLALF18 (2.5:1 molar ratio as in the X-ray diffraction experiments), freeze-fracture electron microscopy

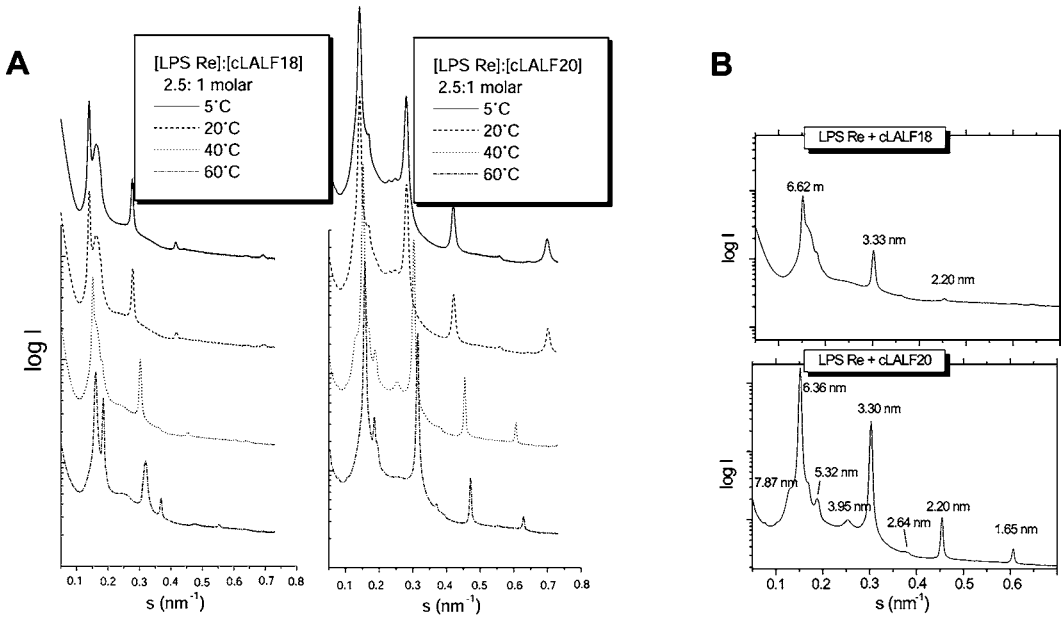

Figure 6 Synchrotron radiation small-angle X-ray diffraction patterns of LPS/peptide mixtures ([LPS]:[cLALF] = 2.5:1 molar ratio)

The scattering vector $s = 1/d = 2\sin\theta/\lambda$ (where d is the spacing ratio, θ the scattering angle and λ the wavelength = 0.15 nm) is plotted against the logarithm of the scattering intensity, log I, (**A**) at different temperatures and (**B**) at 40 °C, both for cLALF18 and 20.

was used. Micrographs are displayed in Figures 7(A)–7(C). For pure LPS, vesicle-like structures are found in the size range 100–200 nm (Figure 7A). The structures, however, often are not closed and form something like 'open eggshells'. When the peptide was added to the LPS, the suspension became turbid with subsequent precipitation. The supernatant (Figure 7B) as well as the precipitate (Figure 7C) were investigated. It can be clearly seen that in the supernatant very large vesicle-like structures and multilamellar stacks are observed apparently due to the formation of fused 'eggshells', with diameters of up to 500 nm. For the precipitate, the morphology completely changes with the occurrence of giant stacks. These stacks corresponded to the multilamellar structures found in the X-ray experiments, with distances between neighbouring stacks in the range 6.3–7.5 nm. Figure 7(C) shows also that in cross-fractured areas stacks with more than 100 single bilayer lamellae can be found.

Intercalation into phospholipid liposomes

A possible intercalation of the peptides or peptide/LPS mixtures into phospholipid membranes were analysed by FRET. As shown in Figure 8 for cLALF9 and cLALF18, the peptides alone (added at $t = 50$ s) were able to intercalate into PS liposomes (increase in FRET signal). When LPS was added subsequently at t = 100 s, there was an additional incorporation, in contrast with added LPS in the absence of the peptide, for which no incorporation was observed (results not shown; see [22]). This means that the peptides acted as a kind of transport molecule similar to that observed for LBP [22].

Finally, when peptides and LPS (peptide/LPS) were incubated before addition to the liposomes, the results indicate a reduced, but still existing membrane incorporation.

Similar results were obtained for all other peptides investigated (results not shown). In some experiments, instead of PS, phospholipids corresponding to the composition of the macrophage membrane ($PL_{M\phi}$) were used. The results were qualitatively the same as with pure PS liposomes, only the observed signal intensities were lower (results not shown).

Inhibition of LPS-induced stimulation of human MNCs

We tested the ability of the peptides to inhibit cell stimulation by LPS Ra from *Salmonella* Minnesota strain R60. Cells were stimulated by LPS alone or pre-incubated with various amounts of peptide (Figure 9). All peptides interacted with LPS, as reflected by a reduction in cell activation. Peptide cLALF12 was able to completely block LPS-induced cell activation (1 ng/ml LPS) at 1 μg/ml. PMB (polymyxin B), the gold standard for cationic LPS-neutralizing peptides, exhibited the same activity at a 10-fold lower concentration.

Cytotoxicity and haemolytic activity

The potential harmful effects of the peptides to human cells were estimated by assessing their cytotoxicity against HeLa cells and their potency to lyse human erythrocytes. At a concentration of 100 μg/ml none of the peptides were cytotoxic and the haemolytic activity was 15 % or below (Table 1).

Antibacterial activity

The antibacterial activity of the peptides was determined first against the LPS-mutant strains *Salmonella* Minnesota R595 and R60 (used for the preparation of the LPS with defined structures used in the experiments described above) grown in LB, a low ionic strength medium that bolsters peptide antimicrobial activity. These experiments suggested that none of the new peptides outperformed the parent peptide cLALF22 (Table 1), but because of the low MIC values obtained under these conditions and with these sensitive LPS mutant strains, we performed additional and more stringent experiments. To this end, we tested the antibacterial activity in Müller–Hinton broth, which is rich in bivalent

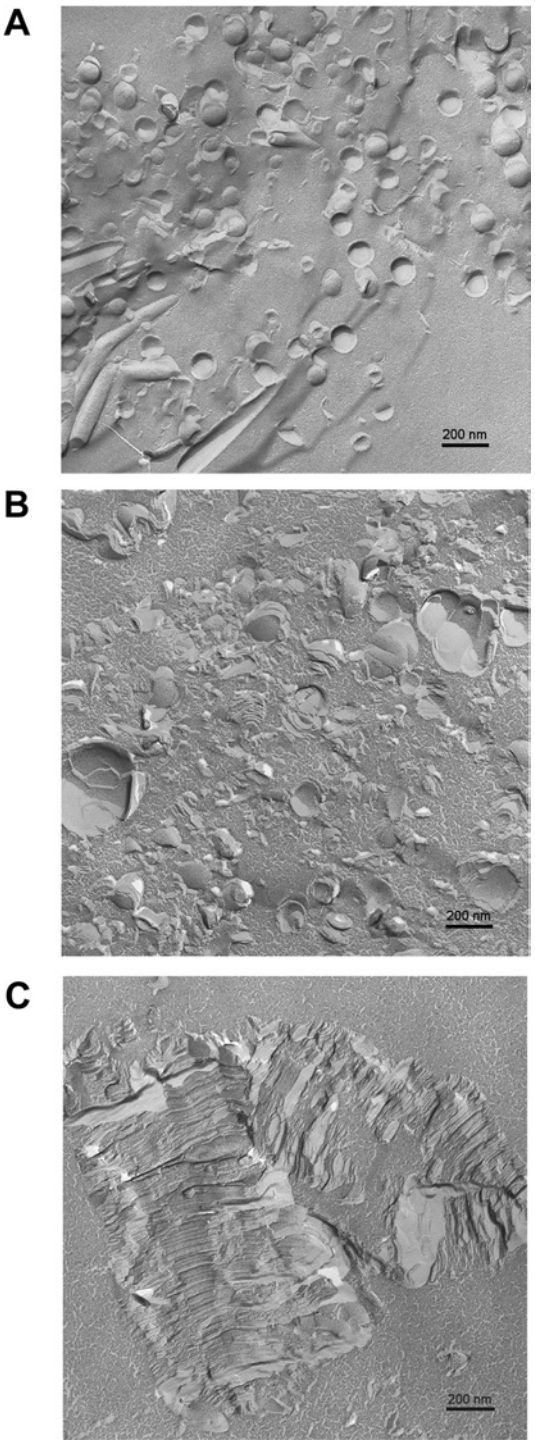

Figure 7 Freeze-fracture electron micrographs of LPS from *Salmonella* Minnesota Re alone (A) and in the presence of cLALF18 ([LPS]:[cLALF] = 3:1) (B) supernatant and (C) precipitation

cations, and using a smooth-type *Escherichia coli* strain and a clinical isolate of *Pseudomonas aeruginosa*, a bacterium with an outer membrane and LPS markedly stabilized by bivalent cations. Under these more stringent conditions, the parent peptide cLALF22 outperformed all the derivatives. This was particularly clear with *Ps. aeruginosa*, highlighting the lack of an effective displacement of bivalent cations from outer membrane and LPS targets by the other peptides (Table 1). It should be mentioned,

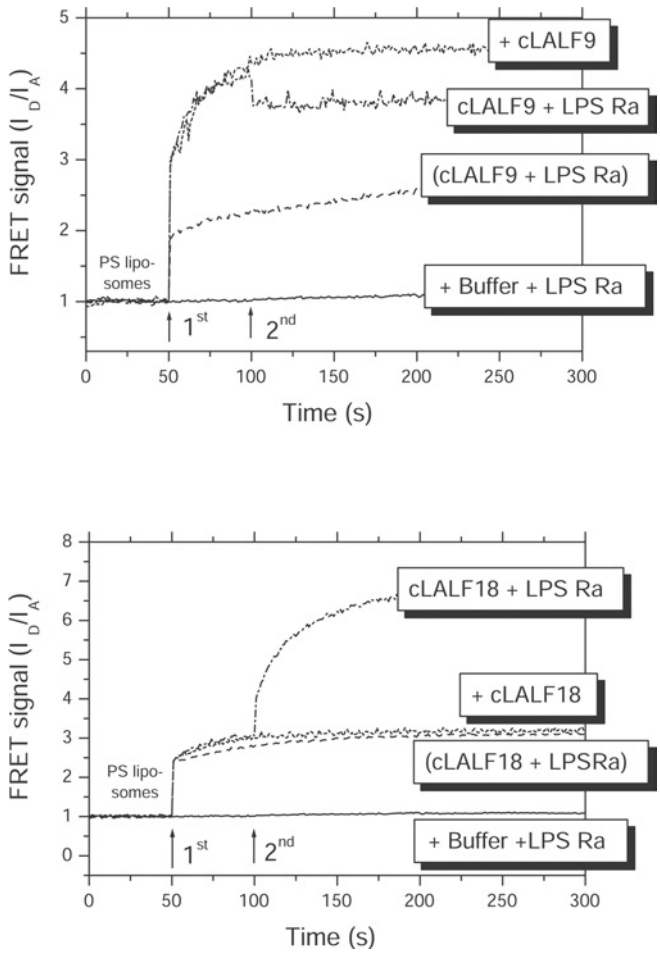

Figure 8 Intercalation of peptide/LPS samples and Hepes buffer control into target cell liposomes made from PS in FRET spectroscopic measurements

Presented is the FRET signal I_D/I_A against time for cLALF9 (upper panel) and cLALF18 (lower panel). The samples were added subsequently at 50 and 100 s to the liposomes.

however, that some of the variants exhibited activity against *Salmonella aureus*. With respect to the most resistant bacterium, i.e. *Ps. aeruginosa*, cLALF9 was the peptide with highest activity beside cLALF22.

DISCUSSION

The development of suitable antimicrobial peptides for a therapy for septic shock and also to fight against local infections is still a challenge in human health care, considering the increase in infectious diseases worldwide and problems such as the emergence of resistances [32]. For these purposes, the development of drugs based on natural endotoxin-binding structures seems a promising approach. This approach comprises, for example, the use of lactoferrin-based [24] and of LALF-based peptides [9]. For synthetic peptides based on the sequence of endotoxin-binding proteins like LALF, it has been shown previously, that some are in principle suitable for application in anti-sepsis research, in particular as they have a sufficiently long half-life in serum [33]. Previously, we have published biophysical data on the interaction of some synthetic cyclic peptides with LPS Re, and reported that certain physicochemical parameters of the LPS Re–peptide interaction correlate with the ability to neutralize LPS [34]. On the basis of these findings, we have constructed several new cyclic

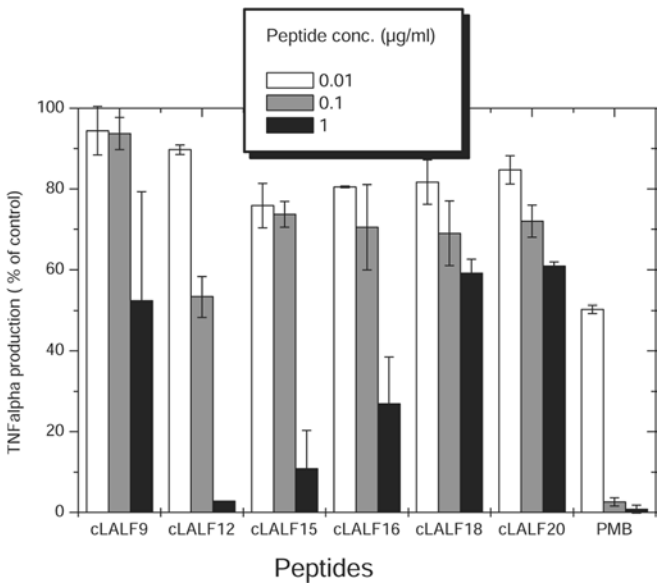

Figure 9 Concentration-dependent inhibition of the biological activity of LPS Ra from *Salmonella* Minnesota strain R60 by synthetic peptides

Peptides were incubated with 1 ng/ml LPS at the indicated peptide concentrations and used to activate human MNCs. As a marker of LPS-induced cell activation, the production of the cytokine TNFα was determined by ELISA. Activation of the cells by LPS alone represents 100 %. PMB served as a control. Results presented are the means for two independent cell stimulations from two different preparations and each stimulation performed in duplicate.

peptides (cLALF 9, 12, 15, 16, 18 and 20). These peptides were designed on the basis of obtaining the hydrophobic cluster at the C-terminus and shortening the peptides stepwise from the N-terminus (Figure 1). We have performed a comprehensive biophysical and biological study of their interaction with the well-characterized endotoxins LPS Re and LPS Ra from *Salmonella* Minnesota strains R595 and R60. Except for the ultrastructural studies in which LPS Re was used, the latter was studied because it has been shown that the endotoxically active unit in natural smooth-form LPS corresponds to an LPS with a complete core oligosaccharide [12].

Our results indicate a strong interaction of the peptides both with bacteria and with isolated LPS. The antibacterial activity of the peptides was clearly more marked on LPS-deficient *Salmonella* mutants in low ionic strength broth than on wild-type clinical isolates in the bivalent-cation rich Müller–Hinton broth. In fact, under the more stringent conditions, only the parent peptide exhibited activity on *Ps. aeruginosa* (Table 1). It should be noted, however, that this bacterium is notoriously refractory to bactericidal peptides under these conditions, and this highlights the activity of cLALF22. On the other hand, the peptides were not cytotoxic and were only slightly haemolytic (Table 1). In a similar way, they were able to inhibit the LPS-induced cytokine production of human MNCs (Figure 9). Very interesting is the dependence of the antibacterial action on the presence of bivalent cations (Müller–Hinton broth). The latter are known to stabilize bacterial outer membranes as well as isolated LPS aggregates [34]. Therefore the action of those peptides that essentially attack the LPS layer of the outer membrane is impeded, which explains the reduction in the MIC/MBC values (Table 1).

The binding of the peptides with LPS shows the following features, which may be relevant for an understanding of the binding to isolated LPS as well as to LPS as a constituent of the outer bacterial membrane.

The binding led to a strong fluidization of the hydrocarbon chains of LPS (Figure 4), with a disappearance of the phase-transition enthalpy (Figures 2 and 3) similar to the observations made for the well-known decapeptide PMB [19]. Concomitantly, a change in the aggregate structures of LPS and lipid A, being unilamellar or mixed unilamellar/inverted cubic in pure form, into multilamellar stacks (Figure 6 and results not shown) was observed, also like PMB. This process is strongly exothermic (Figures 5A and 5B) due to the electrostatic attraction between the negative charges of LPS/lipid A and the positive charges of the peptides (in particular, amino acids arginine and lysine; Figure 1). The enthalpic values (maximum values more than 40 kJ/mol, see Figure 5B) also compare well with those from the interaction of PMB and the nonapeptide PMBN (PMB nonapeptide) with LPS [35].

The electron micrographs (Figure 7) give a clear impression of the underlying morphology, with nearly spherical vesicle-like structures ('open eggshells', Figure 7A) for pure LPS, and very large 'giant' liposomal structures in the supernatant (Figure 7B), apparently due to fusions of the single 'eggshells'. In the precipitate, huge stacks were found (Figure 7C) corresponding to the multilamellae deduced from SAXS (small-angle X-ray scattering) experiments. As already proposed in a preceding paper, the degree of multilamellarization may be a direct measure of the ability of a given peptide to inhibit the LPS-induced cytokine production in MNCs [24]. According to theoretical considerations by Bouwstra et al. [36], from the shapes of the reflections at equidistant ratios, statements about the number of lamellae and size distributions of particles should be possible. Unfortunately, this is apparently valid only for relatively simple situations for pure phospholipids.

Table 1 Antibacterial, cytotoxic and haemolytic activities of cLALF peptides

Antibacterial activity is given as MIC (MBC) in μg/ml and was determined by microdilution assays in (i) 10 % LB/90 % buffer and (ii) Müller–Hinton broth (see the Experimental section). Cytotoxicity against HeLa cells and lysis of human erythrocytes was determined for 100 μg/ml peptide and was calculated relative to an untreated control.

Peptide	*Salmonella* Minnesota R595*	*Salmonella* Minnesota R60*	*E. coli* ATCC 25922†	*Pseudomonas aeruginosa*†	*Salmonella aureus*†	HeLa cells (% cytotoxicity)	Human erythrocytes (% Hb release)
cLALF9	4 (8)	8 (16)	64 (64)	256 (256)	128 (256)	0	9
cLALF12	4 (16)	8 (32)	64 (128)	> 256 (> 256)	64 (128)	0	11
cLALF15	4 (32)	8 (32)	32 (32)	> 256 (> 256)	64 (64)	0	14
cLALF16	4 (16)	16 (32)	64 (64)	> 256 (> 256)	128 (128)	0	15
cLALF18	4 (16)	8 (32)	256 (256)	> 256 (> 256)	256 (256)	0	11
cLALF20	8 (16)	16 (64)	64 (128)	> 256 (> 256)	> 256 (> 256)	0	6
cLALF22	2 (4)	8 (16)	32 (32)	32 (64)	n.d.	0	19

* 10 % LB/90 % buffer.
† Müller–Hinton broth.

For LPS, in cases in which multilamellar aggregates are formed (at low water content and/or high Mg^{2+} concentrations [29,30]), we did not succeed in obtaining this information (J. Andrä, J. Howe and K. Brandenburg, unpublished work). Furthermore, due to the fact that for LPS/peptide mixtures we did not see spherical liposomes but rather relatively different forms in the supernatant and completely different morphologies in the precipitate, the data analysis of Bouwstra et al. [36] is not applicable. Therefore SAXS measurements alone are not sufficient for a complete analysis, and the number of lamellae must be estimated by a different technique, i.e. by analysing the FFTEM pictures. For cLALF18, Figure 7(C) is indicative that stacks with very high numbers of lamellae are formed, and these can be enumerated (most of them are > 100). It is tempting to assume that this is relevant for the interpretation of biological data, since the interaction of LPS with binding proteins such as CD14 and LBP is reduced for stacks with a high number of lamellae as compared with the unilamellar system in the absence of the peptide. Finding a satisfactory explanation for this will be a task for the future.

We have found here a significant increase of the aggregate sizes of LPS (Figure 7C) concomitant with a multilamellarization (Figure 6), in contrast with the findings of Rosenfeld et al. [37], who report that peptides such as human LL-37 and magainin would lead to a dissociation of the LPS aggregates thus preventing them from reacting with LBP or cellular receptors. These authors, however, use more indirect techniques such as flow cytometry with FITC-labelled LPS, which does not represent a direct technique as shown here with the FFTEM method, and furthermore, they have used chemically ill-defined smooth-form LPS which usually consists of a mixture of fractions differing in the length of the sugar chains and the acylation of the lipid A part [12].

It must be emphasized that, except for uncharacterized wild-type LPS [S-LPS (smooth LPS)] in older papers [38], no electron micrographs of chemically characterized endotoxins have ever been published. For lipid A, we have previously characterized the non-lamellar structures using SAXS and FFTEM [39]. A combination of SAXS and cryo-TEM (cryo-transmission electron microscopy) was applied to analyse the interaction of granulysin-derived peptides with endotoxins, in particular with LPS Ra from *Salmonella* Minnesota [40]. The authors found, for pure LPS Ra, fibrillary structures with cylindrical forms with a diameter of the fibrils of 12 nm, whereas in the presence of a granulysin-derived peptide, regularly stacked ribbons emerged, which would correspond to the multilamellar stacks of LPS Re as seen here.

It is important to note that the results of the combined electron microscopy and SAXS measurements presented here allow the unequivocal elucidation of the underlying aggregate structures, which should be of uttermost use in the interpretation of the inhibition activity of the peptides.

For an understanding of the interaction mechanism, the FRET data (Figure 8), which exhibit an intercalation of the peptides into liposomal membranes, are important. This may be of relevance for their antibacterial activity (Table 1) as well for the inhibition of the LPS-induced cytokine expression (Figure 9): for the former, because the bacterial membranes may thus be heavily disturbed in their function, and for the latter, since the uptake of the peptide into the membranes of MNCs can be assumed to be of relevance for their ability to secrete cytokines. There is considerable evidence that the cell activation by LPS starts via a membrane step, induced by binding proteins such as LBP and CD14 [2,41–44]. The detailed mechanisms, however, are not completely resolved. It has been proposed that LBP accelerates the binding of LPS to CD14, and/or that LBP leads to a disintegration, possibly monomerization, of LPS aggregates [2,45], which would imply that the presence of monomers or small aggregates of endotoxin are necessary for endotoxic activity, in accordance with the findings of Takayama et al. [46]. In contrast, Mueller et al. [47,48] showed that aggregates are the biologically active units of endotoxins. We have found that the binding of LBP to LPS leads to a multilamellarization of LPS, which is indicative of an increase rather than a decrease of aggregate sizes as found here for peptide binding (J. Andrä, J. Howe and K. Brandenburg, unpublished work). Independently of this question, it can be stated that LPS incorporated into target cell membranes represents a strong disturbance of the membrane architecture due to the conical geometry (shape) of its lipid A moiety, which triggers cell activation by leading to a conformational change of membrane proteins responsible for cell signalling such as TLR4 [5,49], MaxiK [50], or a complete receptor cluster [51,52]. Since the peptides also incorporate into the membrane, they may be able to change the conical shape of LPS by inducing a lamellar geometry, as was seen in the X-ray diffraction experiments for LPS Re (Figure 6) and lipid A (results not shown).

Conclusions

The ability of the peptides to act antimicrobially and to inhibit the LPS-induced cytokine secretion without exhibiting cytotoxicity and haemolysis makes them or their derivatives potential candidates in sepsis therapy. In the present paper, the biophysical prerequisites for effective endotoxin neutralization have been described: an exothermic reaction between LPS and peptides leading to a fluidization of the lipid A acyl chains with concomitant disappearance of the gel-to-liquid crystalline phase transition, a multilamellarization of the aggregate structure of LPS with a very high number of bilayer stacks, and an incorporation of the peptides into target phospholipids as a model of immune cell membranes.

We are indebted to G. von Busse, U. Diemer, C. Hamann, B. Fölting, K. Stephan and R. Kaiser for technical assistance in the IR spectroscopic, LALF, FRET, DSC, TNFα and FFTEM measurements respectively. The present work has been carried out with financial support from the Commission of the European Communities, specific RTD (Research and Technical Development) programme 'Quality of Life and Management of Living Resources', QLK-CT-2002-01001', 'Antimicrobial endotoxin neutralizing peptides to combat infectious diseases', and from Deutsche Forschungsgemeinschaft SFB 617, 'Molecular mechanisms of epithelial defence' (project A17). Work at the University of Navarra was supported by a grant from the Ministerio de Sanidad y Consumo of Spain (FIS-PI050768).

REFERENCES

1 Tobias, P. S., Soldau, K., Gegner, J. A., Mintz, D. and Ulevitch, R. J. (1995) Lipopolysaccharide binding protein-mediated complexation of lipopolysaccharide with soluble CD14. J. Biol. Chem. **270**, 10482–10488
2 Hailman, E., Lichenstein, H. S., Wurfel, M. M., Miller, D. S., Johnson, D. A., Kelley, M., Busse, L. A., Zukowski, M. M. and Wright, S. D. (1994) Lipopolysaccharide (LPS)-binding protein accelerates the binding of LPS to CD14. J. Exp. Med. **179**, 269–277
3 Gutsmann, T., Haberer, N., Carroll, S. F., Seydel, U. and Wiese, A. (2001) Interaction between lipopolysaccharide (LPS), LPS-binding protein (LBP), and planar membranes. Biol. Chem. **382**, 425–434
4 Akashi, S., Nagai, Y., Ogata, H., Oikawa, M., Fukase, K., Kusumoto, S., Kawasaki, K., Nishijima, M., Hayashi, S., Kimoto, M. and Miyake, K. (2002) Human MD-2 confers on mouse Toll-like receptor 4 species-specific lipopolysaccharide recognition. Int. Immunol. 2001 **13**, 1595–1599
5 Beutler, B. (2000) Endotoxin, Toll-like receptor 4, and the afferent limb of innate immunity. Curr. Opin. Microbiol. **3**, 23–28
6 Rietschel, E. T., Mamat, U., Hamann, L., Wiese, A., Brade, L., Sanchez-Carballo, P., Mattern, T., Zabel, P., Heumann, D., Di Padova, F. et al. (1999) Bacterial endotoxins as inducers of septic shock. Novo Acta Leopoldina **307**, 93–122
7 Heumann, D., Glauser, M. P. and Calandra, T. (1998) Molecular basis of host–pathogen interaction in septic shock. Curr. Opin. Microbiol. **1**, 49–55
8 Andrä, J., Gutsmann, T., Garidel, P. and Brandenburg, K. (2006) Mechanisms of endotoxin neutralization by synthetic cationic compounds. J. Endotoxin Res. **12**, 261–277

9 Andrä, J., Garidel, P., Majerle, A., Jerala, R., Ridge, R., Paus, E., Novitsky, T., Koch, M. H. and Brandenburg, K. (2004) Biophysical characterization of the interaction of *Limulus polyphemus* endotoxin neutralizing protein with lipopolysaccharide. Eur. J. Biochem. **271**, 2037–2046

10 Paus, E. J., Willey, J., Ridge, R. J., Legg, C. R., Finkelman, M. A., Novitsky, T. J. and Ketchum, P. A. (2002) Production of recombinant endotoxin neutralizing protein in *Pichia pastoris* and methods for its purification. Protein Expression Purif. **26**, 202–210

11 Vallespi, M. G., Glaria, L. A., Reyes, O., Garay, H. E., Ferrero, J. and Arana, M. J. (2000) A *Limulus* antilipopolysaccharide factor-derived peptide exhibits a new immunological activity with potential applicability in infectious diseases. Clin. Diagn. Lab. Immunol. **7**, 669–675

12 Jiao, B., Freudenberg, M. and Galanos, C. (1989) Characterization of the lipid A component of genuine smooth-form lipopolysaccharide. Eur. J. Biochem. **180**, 515–518

13 Galanos, C., Lüderitz, O. and Westphal, O. (1969) A new method for the extraction of R lipopolysaccharides. Eur. J. Biochem. **9**, 245–249

14 Holst, O., Suesskind, M., Grimmecke, D., Brade, L. and Brade, H. (1998) Core structures of enterobacterial lipopolysaccharides. Prog. Clin. Biol. Res. **397**, 23–35

15 Ried, C., Wahl, C., Miethke, T., Wellnhofer, G., Landgraf, C., Schneider-Mergener, J. and Hoess, A. (1996) High affinity endotoxin-binding and neutralizing peptides based on the crystal structure of recombinant *Limulus* anti-lipopolysaccharide factor. J. Biol. Chem. **271**, 28120–28127

16 Hoess, A., Watson, S., Siber, G. R. and Liddington, R. (1993) Crystal structure of an endotoxin-neutralizing protein from the horseshoe crab, *Limulus* anti-LPS factor, at 1.5 A resolution. EMBO J. **12**, 3351–3356

17 Blume, A. and Garidel, P. (1999) Lipid model membranes and biomembranes. In From Macromolecules to Man (Kemp, R. B., ed.), pp. 109–173, Elsevier, Amsterdam

18 Garidel, P., Rappolt, M., Schromm, A. B., Howe, J., Lohner, K., Andrä, J., Koch, M. H. and Brandenburg, K. (2005) Divalent cations affect chain mobility and aggregate structure of lipopolysaccharide from *Salmonella minnesota* reflected in a decrease of its biological activity. Biochim. Biophys. Acta **1715**, 122–131

19 Brandenburg, K., Moriyon, I., Arraiza, M. D., Lehwark-Yvetot, G., Koch, M. H. J. and Seydel, U. (2002) Biophysical investigations into the interaction of lipopolysaccharide with polymyxins. Thermochim. Acta **382**, 189–198

20 Koch, M. H. J. and Bordas, J. (1983) X-ray diffraction and scattering on disordered systems using synchrotron radiation. Nucl. Instr. Methods **208**, 461–469

21 Brandenburg, K., Funari, S. S., Koch, M. H. J. and Seydel, U. (1999) Investigation into the acyl chain packing of endotoxins and phospholipids under near physiological conditions by WAXS and FTIR spectroscopy. J. Struct. Biol. **128**, 175–186

22 Schromm, A. B., Brandenburg, K., Rietschel, E. Th., Flad, H.-D., Carroll, S. F. and Seydel, U. (1996) Lipopolysaccharide binding protein (LBP) mediates CD14-independent intercalation of lipopolysaccharide into phospholipid membranes. FEBS Lett. **399**, 267–271

23 Brandenburg, K., Garidel, P., Andrä, J., Jürgens, G., Müller, M., Blume, A., Koch, M. H. J. and Levin, J. (2003) Cross-linked hemoglobin converts endotoxically inactive pentaacyl endotoxins into a physiologically active conformation. J. Biol. Chem. **278**, 47660–47669

24 Andrä, J., Lohner, K., Blondelle, S. E., Jerala, R., Moriyon, I., Koch, M. H., Garidel, P. and Brandenburg, K. (2005) Enhancement of endotoxin neutralization by coupling of a C12-alkyl chain to a lactoferricin-derived peptide. Biochem. J. **385**, 135–143

25 Martinez de Tejada, G., Pizarro-Cerda, J., Moreno, E. and Moriyon, I. (1995) The outer membranes of *Brucella* spp. are resistant to bactericidal cationic peptides. Infect. Immun. **63**, 3054–3061

26 Brandenburg, K., Jürgens, G., Andrä, J., Lindner, B., Koch, M. H. J., Blume, A. and Garidel, P. (2002) Biophysical characterization of the interaction of high-density lipoprotein (HDL) with endotoxins. Eur. J. Biochem. **269**, 5972–5981

27 Brandenburg, K., Andrä, J., Müller, M., Koch, M. H. J. and Garidel, P. (2003) Physicochemical properties of bacterial glycopolymers in relation to bioactivity. Carbohydr. Res. **338**, 2477–2489

28 Rietschel, E. T., Brade, H., Holst, O., Brade, L., Müller-Loennies, S., Mamat, U., Zähringer, U., Beckmann, F., Seydel, U., Brandenburg, K. et al. (1996) Bacterial endotoxin: chemical constitution, biological recognition, host response, and immunological detoxification. Curr. Top. Microbiol. Immunol. **216**, 39–81

29 Brandenburg, K., Koch, M. H. J. and Seydel, U. (1992) Phase diagram of deep rough mutant lipopolysaccharide from *Salmonella minnesota* R595. J. Struct. Biol. **108**, 93–106

30 Seydel, U., Koch, M. H. J. and Brandenburg, K. (1993) Structural polymorphisms of rough mutant lipopolysaccharides Rd to Ra from *Salmonella minnesota*. J. Struct. Biol. **110**, 232–243

31 Brandenburg, K., Koch, M. H. J. and Seydel, U. (1990) Phase diagram of lipid A from *Salmonella minnesota* and *Escherichia coli* rough mutant lipopolysaccharide. J. Struct. Biol. **105**, 11–21

32 Hancock, R. E. W. and Sahl, H.-G. (2006) Antimicrobial and host-defense peptides as new anti-infective therapeutic strategies. Nat. Biotechnol. **24**, 1551–1557

33 Dankesreiter, S., Hoess, A., Schneider-Mergener, J., Wagner, H. and Mietke, T. (2000) Synthetic endotoxin-binding peptides block endotoxin-triggered TNF-α production by macrophages *in vitro* and *in vivo* and prevent endotoxin-mediated toxic shock. J. Immunol. **164**, 4804–4811

34 Andrä, J., Lamata, M., Martinez de Tejada, G., Bartels, R., Koch, M. H. J. and Brandenburg, K. (2004) Cyclic antimicrobial peptides based on *Limulus* anti-lipopolysaccharide factor for neutralization of lipopolysaccharide. Biochem. Pharmacol. **68**, 1297–1307

35 Brandenburg, K., David, A., Howe, J., Koch, M. H., Andrä, J. and Garidel, P. (2005) Temperature dependence of the binding of endotoxins to the polycationic peptides polymyxin B and its nonapeptide. Biophys. J. **88**, 1845–1858

36 Bouwstra, J. A., Gooris, G. S., Bras, W. and Talsma, H. (1993) Small angle X-ray scattering: possibilities and limitations in characterization of vesicles. Chem. Phys. Lipids **64**, 83–98

37 Rosenfeld, Y., Papo, N. and Shai, Y. (2006) Endotoxin (lipopolysaccharide) neutralization by innate immunity host-defense peptides. J. Biol. Chem. **281**, 1636–1643

38 Shands, J. W. (1971) The physical structure of bacterial lipopolysaccharides. In Microbial Toxins, Vol. 4: Bacterial Endotoxins (Weinbaum, G., Kadis, S. and Ajl, S. J., eds.), pp. 127–144, Academic Press, New York and London

39 Brandenburg, K., Richter, W., Koch, M. H. J., Meyer, H. W. and Seydel, U. (1998) Characterization of the nonlamellar cubic and H_{II} structures of lipid A from *Salmonella enterica* serovar Minnesota by X-ray diffraction and freeze-fracture electron microscopy. Chem. Phys. Lipids **91**, 53–69

40 Chen, X., Howe, J., Andrä, J., Rössle, M., Richter, M., Galvao da Silva, A. P., Krensky, A. M., Clayberger, C. and Brandenburg, K. (2007) Biophysical analysis of the interaction of granulysin-derived peptides with enterobacterial endotoxins. Biochim. Biophys. Acta, in the press

41 Pugin, J., Schürer-Maly, C. C., Leturcq, D., Moriarty, A., Ulevitch, R. J. and Tobias, P. S. (1993) Lipopolysaccharide activation of human endothelial and epithelial cells is mediated by lipopolysaccharide-binding protein and soluble CD14. Proc. Natl. Acad. Sci. U.S.A. **90**, 2744–2748

42 Tapping, R. I. and Tobias, P. S. (1997) Cellular binding of soluble CD14 requires lipopolysaccharide (LPS) and LPS-binding protein. J. Biol. Chem. **272**, 23157–23164

43 Ulevitch, R. J. and Tobias, P. S. (1999) Recognition of Gram-negative bacteria and endotoxin by the innate immune system. Curr. Opin. Immunol. **11**, 19–22

44 Gutsmann, T., Schromm, A. B., Koch, M. H. J., Kusumoto, S., Fukase, K., Oikawa, M., Seydel, U. and Brandenburg, K. (2000) Lipopolysaccharide-binding protein-mediated interaction of lipid A from different origin with phospholipid membranes. Phys. Chem. Chem. Phys. **2**, 4521–4528

45 Tobias, P. S., Soldau, K., Iovine, N. M., Elsbach, P. and Weiss, J. (1997) Lipopolysaccharide (LPS)-binding proteins BPI and LBP form different types of complexes with LPS. J. Biol. Chem. **272**, 18682–18685

46 Takayama, K., Mitchell, D. H., Din, Z., Mukerjee, P., Li, C. and Coleman, D. L. (1994) Monomeric Re lipopolysaccharide from *Escherichia coli* is more active than the aggregated form in the *Limulus* amebocyte lysate assay and in inducing Egr-1 mRNA in murine peritoneal macrophages. J. Biol. Chem. **269**, 2241–2244

47 Mueller, M., Lindner, B., Dedrick, R., Schromm, A. B. and Seydel, U. (2005) Endotoxin: physical requirements for cell activation. J. Endotoxin Res. **11**, 299–303

48 Mueller, M., Lindner, B., Kusumoto, S., Fukase, K., Schromm, A. B. and Seydel, U. (2004) Aggregates are the biologically active units of endotoxins. J. Biol. Chem. **279**, 26307–26313

49 Qureshi, S. T., Lariviere, L., Leveque, G., Clermont, S., Moore, K. J., Gros, P. and Malo, D. (1999) Endotoxin-tolerant mice have mutations in Toll-like receptor 4 (*Tlr4*). J. Exp. Med. **189**, 615–625

50 Blunck, R., Scheel, O., Müller, M., Brandenburg, K., Seitzer, U. and Seydel, U. (2001) New insights into endotoxin-induced activation of macrophages: involvement of a K^+ channel in transmembrane signaling. J. Immunol. **166**, 1009–1015

51 Triantafilou, K., Triantafilou, M. and Dedrick, R. L. (2001) A CD14-independent LPS receptor cluster. Nat. Immunol. **2**, 338–345

52 Triantafilou, M., Brandenburg, K., Kusumoto, S., Fukase, K., Mackie, A., Seydel, U. and Triantafilou, K. (2004) Combinational clustering of receptors following stimulation by bacterial products determines LPS responses. Biochem. J. **381**, 527–536

Received 22 February 2007/11 May 2007; accepted 14 May 2007
Published as BJ Immediate Publication 14 May 2007, doi:10.1042/BJ20070279